

Elucidation of Reaction Behaviors in Sonocatalytic Decolorization of Amaranth Dye in Water Using Zeolite Y Co-Incorporated with Fe and TiO₂

Atheel Hassan Alwash^{1,2*}, Ahmad Zuhairi Abdullah¹, Norli Ismail³

¹School of Chemical Engineering, Universiti Sains Malaysia, Penang, Malaysia

²Department of Chemistry, College of Science, Al-Nahrain University, Baghdad, Iraq

³School of Industrial Technology, Universiti Sains Malaysia, Penang, Malaysia

Email: *atheel_eng78@yahoo.com

Received February 2, 2013; revised March 2, 2013; accepted March 25, 2013

Copyright © 2013 Atheel Hassan Alwash *et al.* This is an open access article distributed under the Creative Commons Attribution License, which permits unrestricted use, distribution, and reproduction in any medium, provided the original work is properly cited.

ABSTRACT

The Zeolite Y as a support was modified by the incorporating of Fe and TiO₂ in one single step using impregnation method. The synergistic effects between those components enhance the catalytic activity for the degradation of amaranth dye under ultrasonic irradiation with output power of 50 W and 40 kHz frequency. Different characterization techniques were used to elucidate the physical and chemical properties of the produced catalysts. The XRD results indicated that the type of titanium precursor significantly effects on the crystallinity of 0.4% Fe/15%TiO₂-NaY catalyst. The AFM results detected that the TiO₂ formed a layer covered the surface of zeolite while Fe clusters were located close to TiO₂. The influence of reaction parameters such as TiO₂ and Fe content, pH values, amount of hydrogen peroxide used, catalyst loading and the initial dye concentration were investigated for the decolorization efficiency of amaranth. The maximum decolorization efficiency for 0.4%Fe/15%TiO₂-NaY was 100% after 120 min of reaction time with an initial dye concentration of 30 mg/L, 2 g/L of catalyst loading, natural pH about 5.5 and 0.65 mM H₂O₂.

Keywords: Dye Degradation; Impregnation Method; Incorporation of Metals

1. Introduction

Dyes with their structural variety have been used as important raw materials for colorants in different industries, such as textiles, rubber, leather, paper, food and plastic. Large quantities of aqueous waste and dye effluents are produced during processing operations [1]. The high stability of the dyestuffs makes them resistance to the conventional treatment processes and limited their biodegradation. Thus advanced oxidation processes (AOPs) such as ultrasonic process have been widely investigated to overcome the drawbacks of the traditional methods.

The synergetic effect between ultrasonic irradiation and heterogeneous catalyst such as titanium oxide enhance the activity of the process due to the generation of more hydroxyl radicals species. However, the separation difficulties for the superfine TiO₂ particles after the reaction makes the efforts focused on the immobilization of TiO₂ on different types of support [2]. Zeolite support has been investigated extensively for the immobilization

of TiO₂ especially for photocatalytic application due to its special properties such as the presence of Lewis acid and Lewis base sites in the framework that play an important role in charge transfer and electron transfer processes [3,4].

Our previous work [5] reported the successful results for the catalytic activity of Fe loaded on TiO₂ encapsulated zeolite for the degradation of dye under ultrasonic reaction. The position of TiO₂ in the previous study was encapsulated into the pores of zeolite using ion-exchange method while the Fe was located at the external surface of zeolite using impregnation method. Therefore, it was of great interest to examine the variations occurs in characteristic and catalytic activity of the produced catalyst by replacing the position of TiO₂ to be located at the external surface of zeolite together with Fe under ultrasonic reaction. The selection of ultrasonic-assisted process should provide an efficient activity to the waste water treatment process due to the strong penetration ability of ultrasound in water which can usually reach 20 - 30 cm from the energy source [6].

*Corresponding author.

The co-incorporation of TiO₂ and Fe with zeolite structure should enhance the sonocatalytic activity since more active sites will be provided in the reaction. Furthermore, using zeolite as a support for these metals was ascribed to its high surface area and its ability to act as a host for more than one active component. Different characterization techniques have been used to elucidate the physical and chemical properties of the produced catalysts. The sonocatalytic activity has been investigated as a function of different reaction parameters such as solution acidity, catalyst loading, the addition of H₂O₂ and the effect of initial dye concentration for the decolorization of amaranth dye which has been used as the probe molecule in this study.

2. Experimental

2.1. Materials

H-Y zeolite with Si/Al 15 was obtained from Zeolyst International while amaranth dye was purchased from Sigma. Meanwhile, potassium titanoxalate dehydrate and sodium chloride crystals were supplied by J. T. Baker while iron (III) nitrate nonhydrate was obtained from Merck Sdn. Bhd. Hydrogen peroxide (35%) used to accelerate the reaction was supplied by R&M Chemicals.

2.2. Catalyst Preparation Method

2.2.1 Preparation of NaY

Dried H-Y zeolite was first converted to its sodium form by means of an ion-exchange method [7]. The zeolite was washed with 1 M NaCl at 80°C for 4 h in such a way that the ratio of zeolite to sodium chloride solution was 1:80. The slurry was then filtered and washed with deionized water to remove the excess amount of NaCl. In order to achieve complete exchange of sodium into the zeolite, the above cycle was repeated twice. The sample was then dried for 12 h at a temperature of 80°C and then calcined in a muffle furnace at 550°C for 5 h.

2.2.2. Incorporation of Fe and TiO₂ with NaY

The heterogeneous catalyst was prepared using the procedure reported by Li *et al.* [8]. One gram of NaY was suspended in 50 mL water and known amounts of Fe (NO₃)₃ (Fe³⁺ loading from 0.2 - 0.6 wt%) and fixed amount of titanium precursor (the theoretical proportion of TiO₂ in the catalyst is 15 wt% TiO₂) was added into the suspended solution and mixed by mechanical stirrer for 24 h at ambient temperature. The resulting samples were then dried using a rotary evaporator and placed in an oven at 100°C for 4 h. Then, the produced solids were calcined at 550°C for 5 h. The produced catalysts were denoted as *x* Fe%/15%TiO₂-NaY where *x* is the wt% of Fe. In order to investigate the effect of TiO₂ with fixed amount of Fe, the same preparation method was repeated

with TiO₂ loading from 5 - 20 wt% and fixed amount of Fe.

2.3. Catalytic Characterization

Characterization of the catalysts with different analytical techniques was performed to elucidate the incorporation of Ti and Fe species with the framework of Na-Y. Among various catalysts loadings, the best catalyst was demonstrated by activity of 0.4% Fe/15%TiO₂-NaY. Thus it was chosen to completely characterize. The crystalline structure of the obtained catalysts was investigated by means of X-ray diffraction using an XRD system (Philips Goniometer PW 1820). The Fourier transforms infrared spectrometry (Perkin Elmer) was carried out with wave number range between (400 - 4000) cm⁻¹. Transmission electron microscope (TEM) images were obtained using a Phillips CM 12 transmission electron microscope equipped with an image analyzer and operated at 120 kV. Finally, the roughness of the catalyst surface was investigated using SPA 400 atomic force microscopy (AFM) technique.

2.4. Sonocatalytic Reaction

All sonocatalytic experiments were carried out in a 250 mL cylindrical vessel and placed in an ultrasonic bath (Cole-Parmer) for up to 120 min. Before starting the ultrasonic reaction, the solution was stirred for 30 min at room temperature to maintain the good dispersion of catalyst with the dye solution. The experimental conditions were set at an initial amaranth dye concentration of 10 mg/L, a catalyst amount of 1.5 g/L and the solution pH was kept at its original level without any adjustment. The ultrasonic output power was fixed at 50 W with a frequency of 40 kHz. The decolorization efficiency was calculated based on UV-vis spectrophotometer results. The concentration of the dye solution was determined at its maximum absorbance wavelength of 521 nm. The decolorization efficiency of the catalyst was calculated based to the following equation;

$$\text{Decolorization (\%)} = \left[1 - \frac{C_t}{C_0} \right] \times 100\% \quad (1)$$

where, *C*₀ (mg/L) is the initial concentration of dye and *C*_{*t*} (mg/L) is the concentration of dye at certain reaction time, *t*(min).

3. Results and Discussion

3.1. Characterization of the Catalyst

3.1.1. XRD

The XRD pattern of NaY, potassium titanium oxalate (PTO) calcined at 550°C, 0.4% Fe-NaY, 15% TiO₂-NaY and 0.4% Fe/15%TiO₂-NaY are shown in **Figure 1**. The

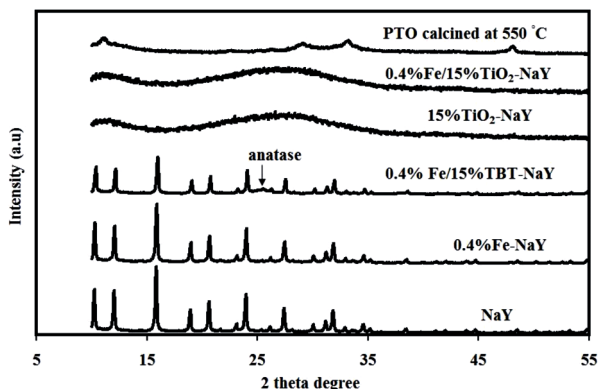


Figure 1. X-ray diffraction patterns of different catalysts used in this study.

parent NaY shows high crystalline structure while the calcined PTO showed an amorphous structure with small anatase peak at 2θ 48.1° . However, after the incorporation of Fe and TiO_2 with NaY for the case of 0.4% Fe/15% TiO_2 -NaY, the crystallinity of zeolite disappeared and a single wide peak with low intensity appeared at 2θ of 27.7° ascribed to rutile phase. The formation of new material after the incorporation of Fe/ TiO_2 with zeolite was not suggested since the diffraction pattern of 0.4% Fe/15% TiO_2 -NaY was similar to that of 15% TiO_2 -NaY catalyst.

No characteristic peak for iron oxide phase that could be formed after the calcination step was detected either for 0.4% Fe-NaY or 0.4% Fe/15% TiO_2 -NaY. This could be ascribed to the low loading of Fe used in this study. Castano *et al.* [9] reported that the unclear diffraction for some metals could be attributed to the small crystal size (<4 nm) or to the well-dispersion of amorphous phases that caused unclear detection by XRD. Wang *et al.* [10] did not indicate any clear peak for Fe phases after the doping of TiO_2 and Fe into a natural zeolite even at higher concentrations up to 7% mol of Fe.

It has been reported in literature that the transformation phase temperature from anatase to rutile usually occurs at temperature between 700°C - 800°C [11,12]. Therefore, the appearance of the rutile phase for both catalysts *i.e.* 15% TiO_2 -NaY and 0.4% Fe/15% TiO_2 -NaY should not be attributed to the calcination temperature used in this study. However, the titanium precursor could be the reason behind the appearance of rutile phase since no anatase peak at 25.1° (highest peak for anatase phase) was detected in the bare potassium titanium oxalate (PTO) diffraction calcined at 550°C .

In order to investigate the effect of titanium precursor on the crystallinity of zeolite, the titanium precursor was changed with another organic precursor *i.e.* tetra butyl orthotitanate (TBT) using the same preparation method and the catalyst was denoted as 0.4% Fe/15% TBT-NaY as shown in **Figure 1**. The result indicated that zeolite

support was able to retain its crystallinity even after the loading of both Fe and TiO_2 and a small anatase peak was detected at 25.1° . As a result, it seemed that the dispersion of TiO_2 clusters with zeolite depend on the type of titanium precursor and consequently affecting on the crystallinity of the support. The partial incorporation between Ti species and the framework of zeolite might be occurred during the preparation method since the zeolite structure have super cages and pore size of 1.3 nm and 0.74 nm, respectively. The excess amount of Ti species could be anchored on the surface of the support after the calcination step thus lead to a significant reduction in the crystallinity of catalyst due to the accumulation of TiO_2 phase on it.

3.1.2. Fourier Transforms Infrared Spectrometry

The FTIR spectra for the parent NaY, 0.4% Fe-NaY, 15% TiO_2 -NaY and 0.4% Fe/15% TiO_2 -NaY are presents in **Figure 2**. The absorption features of NaY resulted in different absorption peaks in the range between ($4000 - 400$) cm^{-1} . The peak at 3439 cm^{-1} and 1626 cm^{-1} represents the presence of water molecules or hydroxyl groups attached to zeolite structure. Hassan and Hameed [13] reported that the region from 1600 to 3700 cm^{-1} is ascribed to the existence of zeolite water molecules. These water molecules attached to the silicate minerals can be found in two types *i.e.* intact molecules or as OH groups formed from the dissociation of water interact with metals such as (Si^{4+} , Al^{3+}). The peak at 1138 cm^{-1} was ascribed to the asymmetric stretching modes of internal tetrahedral. While the absorption peak at 514 and 450 cm^{-1} represent the T-O bending vibrations of internal tetrahedral in zeolite [14]. The zeolite framework also present peak around 1050 cm^{-1} ascribed to Si-O-Si asymmetric stretching mode of external linkages bond in zeolite framework. It should be mentioned that the terms internal and external vibrations have been used in FTIR spectroscopy for zeolites materials to describe the vibrations in tetrahedral building units and between them [15].

A significant change in stretching vibration for 15%

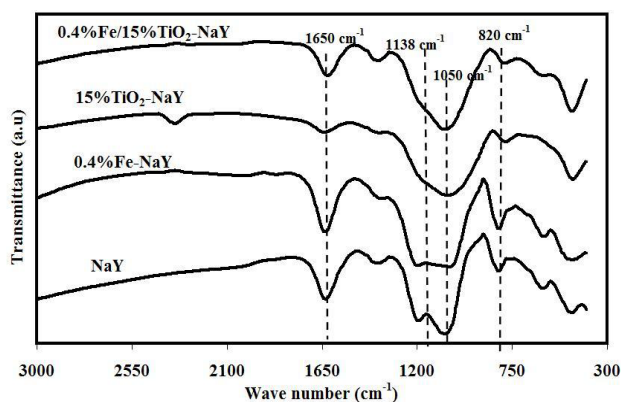


Figure 2. FTIR spectrum of different types of catalysts.

TiO₂-NaY and 0.4% Fe/15% TiO₂-NaY in comparative to NaY was observed at peak value around 1650 cm⁻¹ ascribed to the existence of water molecules in zeolite [13]. Nikazar *et al.* [16] reported that the changes occurs in this regions after the doping of metal indicated that a certain amount of OH was demolished by this metal *i.e.* Ti and Fe. The peaks at 1138 cm⁻¹ and 1050 cm⁻¹ for NaY were attributed to the asymmetric stretching modes of internal tetrahedral and asymmetric stretching of external linkage for (T-O-T) respectively [17]. However, the peak at 1138 cm⁻¹ (NaY) was disappeared in the case of 15% TiO₂-NaY and 0.4% Fe/15% TiO₂-NaY due to the effect of TiO₂ and Fe loading. Accordingly, the change occurred in peak at 1050 cm⁻¹ was ascribed to the sensitivity of this region to the structure changes.

No peak could be detected at 960 cm⁻¹ for 15% TiO₂-NaY and 0.4% Fe/15% TiO₂-NaY after the loading of TiO₂ which was assigned to the anti-symmetric stretching vibration of the Ti-O-Si [18]. This peak was ascribed to the interaction of Ti species with the internal framework of zeolite. However, the absence of this peak in this catalyst suggests the dispersion of TiO₂ to be more on the external surface of zeolite. This result is in agreement with the results obtained by XRD.

Quintero Ortíz *et al.* [19] reported that the peak in NaY at 820 cm⁻¹ was assigned to the stretching vibrations of external bond between tetrahedral of zeolite. However, this peak showed a reduction in stretching vi-

bration and shifting to lower wavelength after the incorporation of TiO₂ for the case of 15% TiO₂-NaY and 0.4% Fe/15% TiO₂-NaY. While no changes were detected for the case of 0.4% Fe-NaY so, this change was ascribed to the incorporation of TiO₂. On the other hand, the stretching vibration from 500 to 700 cm⁻¹ was ascribed to the sensitive change in the pseudo- lattice vibration of zeolite after the loading of Metal/Zeolite [20]. From the above analysis, the differences in FTIR spectra were evident especially for TiO₂ loading due to its higher amount in comparative to Fe.

3.1.3. AFM Technique

The morphological characteristics was investigated based on the values of mean roughness that were presented in two and three dimensional AFM images of NaY, 15% TiO₂-NaY, 0.4% Fe-NaY and 0.4% Fe/15% TiO₂-NaY as in **Figure 3**. The variation occurred in surface morphology of the prepared catalysts suggested the significant effect of Ti and Fe incorporated with zeolite. The results for the degree of roughness was in the sequence of NaY > 0.4% Fe-NaY > 0.4% Fe/15% TiO₂-NaY > 15% TiO₂-NaY with roughness values of 74 nm, 72 nm, 48 nm and 44 nm, respectively. The similarity in the roughness of the catalyst surface between NaY and 0.4% Fe-NaY seemed to be due to the low loading of the Fe₂O₃ which might be formed after the calcination step. Thus, showed this slight effect on the uniformity on the catalyst surface.

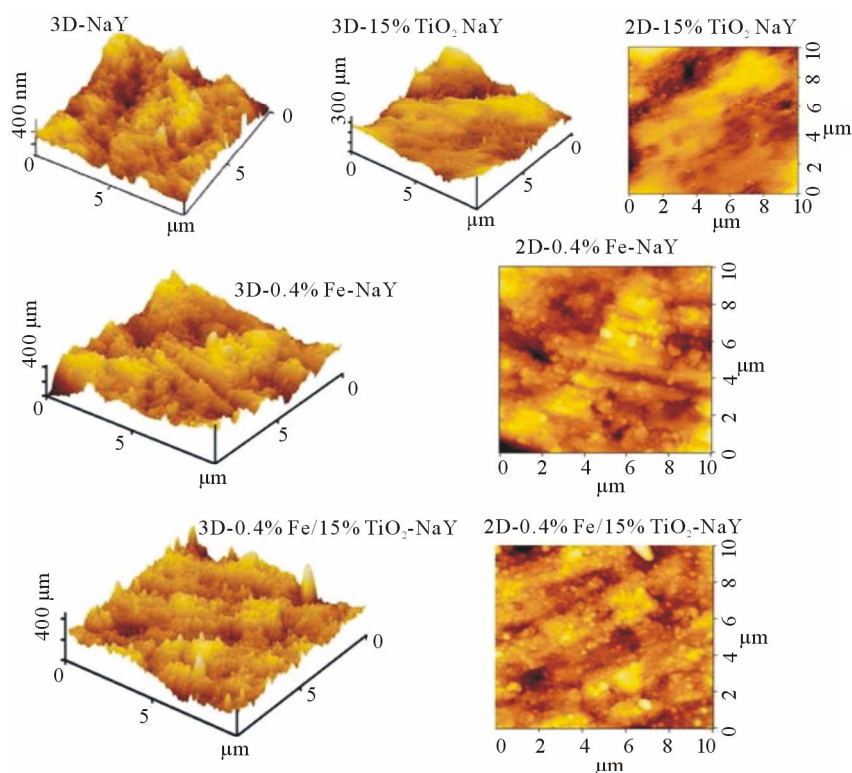


Figure 3. Two and three dimension AFM images for different types of catalyst used.

However, it was clear that the roughness of the catalyst was significantly decreased after the loading of TiO_2 for both cases of 15% TiO_2 -NaY and 0.4% Fe/15% TiO_2 -NaY. This extreme reduction in the roughness of the catalysts surfaces were ascribed to the small crystal size of the supported TiO_2 which was in agreement with XRD results (low intensity and wide peak). Although, the AFM technique can not differentiate between the existing metal on the surface of the catalyst. However, small clusters were significantly detected for the case of 0.4% Fe/15% TiO_2 -NaY which could be ascribed to Fe oxide formed after the calcination step. While for the case of 15% TiO_2 -NaY, it was clear that TiO_2 phase formed a layer covered the surface of zeolite and no small clusters were observed on its surface comparing to that of 0.4% Fe/15% TiO_2 -NaY.

3.1.4. Transmission Electron Microscope

The TEM imaging was carried out for parent NaY, and 0.4% Fe/15% TiO_2 -NaY catalysts. The unmodified zeolite structure can be observed in **Figures 4(a)** and **(b)** for two different magnifications *i.e.* 8 kX and 45 kX, respectively. The hexagonal crystalline geometry of the zeolite remained virtually unchanged for the case of 0.4% Fe/15% TiO_2 -NaY using impregnation method as was observed in **Figure 4(c)**. These results proved that the zeolite was generally able to maintain its original structure after the loading of TiO_2 and Fe since no significant damages were detected on its hexagonal structure. The TEM image suggested that the position of TiO_2 clusters were mainly positioned on the external surface of zeolite due to appearance of many white clusters accumulated on the external surface of zeolite structure and it was not shielded by zeolite particles. However, it was not possible to detect the Fe metal due to the higher loading of TiO_2 that was significantly occupied the surface of zeolite.

3.2. Sonocatalytic Degradation Process

3.2.1. Effect of Incorporation of Fe and Fixed Amount of TiO_2 with Zeolite

In order to obtain higher decolorization activity of the catalyst, preliminary experiments were carried out to investigate the synergistic effect between different wt% of Fe with fixed amount of TiO_2 15 wt% as shown in **Figure 5**. The experimental runs were carried out with 10 mg/L initial dye concentration, catalyst loading of 1.5 g/L and natural pH about 5.5 without the addition of H_2O_2 in the reaction. The results showed that the catalytic activity significantly increased with increasing the wt% of Fe loading from 0.2% to 0.4% Fe with catalytic activities of 54% and 76%, respectively. In this reaction, the Fe acted as electron acceptor from the e^- - h^+ pairs generated through the activation of TiO_2 in the zeolite.

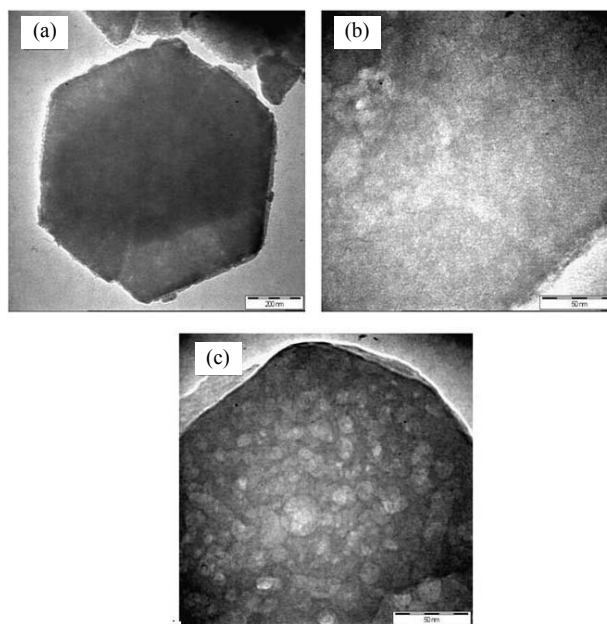


Figure 4. TEM images for (a) and (b) NaY and (c) 0.4% Fe/5% TiO_2 -NaY.

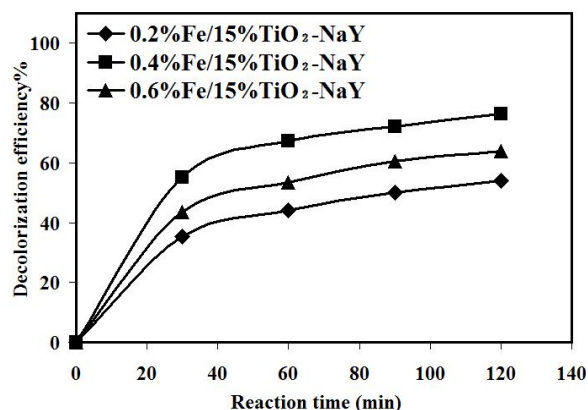


Figure 5. Effect of interaction between different loadings of Fe and fixed amount of TiO_2 with zeolite.

Increasing the loading amount of Fe would provide more electron traps to hinder e^- - h^+ ions recombination leading to an increase in the sonocatalytic activity. In a complementary role, the zeolite support worked as a hole trap thus enhance efficiently the inhibition of the electron hole recombination. Therefore, the lower catalytic activity for the catalyst at 0.2% Fe loading was ascribed to the insufficient amount of Fe ions to inhibit the e^- - h^+ recombination. However, with increasing loading of Fe up to 0.6 wt%, the catalytic activity was found to decrease to 64%. In this case, as the wt% Fe was further increased, the e^- - h^+ recombination rate would increase also due to the existence of excess amount of Fe which would act as a charge carrier to cause this reduction in the catalytic activity. Bajamundi *et al.* [21] investigated the effect of Fe loading from 0 - 3.0 wt% Fe on the activ-

ity of $\text{TiO}_2/\text{Al}_2\text{O}_3$ and the higher degradation efficiency of methylene blue was at 0.1% Fe. As a conclusion it seems that increasing the concentration of Fe up to 0.4 wt% showed significant enhance in catalytic activity and the addition of higher concentration affected negatively on catalytic activity.

3.2.2. Effect of Incorporation of TiO_2 and Fixed Amount of Fe with Zeolite on Sonocatalytic Activity

As the optimum loading of Fe was 0.4 wt%, further experiment runs were carried out to investigate the interaction between fixed loading of 0.4% Fe with different loadings of TiO_2 from 5 - 20 wt% and the results are shown in **Figure 6**. The sonocatalytic activity was found to increase with increasing the loading of TiO_2 from 5 - 15 wt% reaching its maximum activity of 76% at the highest TiO_2 loading. Increasing the loading of TiO_2 would provide more active sites to enhance the generation of $\cdot\text{OH}$ radicals during the sonocatalytic reaction [11]. Further increase in TiO_2 loading above the optimum value *i.e.* 20 wt%, the decolorization efficiency of amaranth was significantly decreased to 34%. This drastic reduction in catalytic activity might be ascribed to the aggregation of TiO_2 clusters on the surface of zeolite [20]. Furthermore, with increasing amount of TiO_2 , the amount of available Fe sites would not be sufficient to inhibit the e^-h^+ recombination thus, reduced the catalytic activity of the catalyst.

Another factor that can negatively effect on the catalytic activity might be referring to the formation of a separate TiO_2 phase with increasing the TiO_2 loading. This phase will no longer be incorporated with zeolite framework consequently, cause this reduction in catalytic activity. This result was suggested based on the results obtained from the AFM analysis since, there was a thin layer covered the surface of zeolite after the loading of 15 wt% of TiO_2 . However, the incorporation of 0.4% of Fe/15% TiO_2 with zeolite showed the higher catalytic

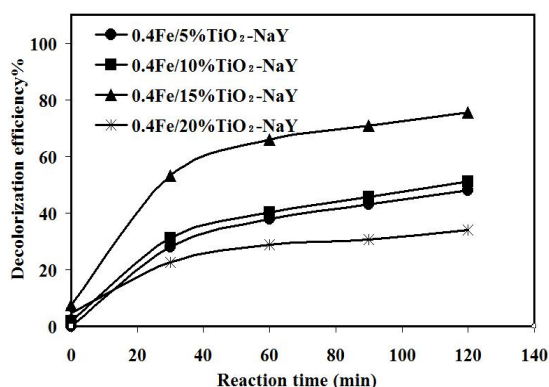


Figure 6. Effect of interaction of different loadings of TiO_2 and fixed amount of Fe with zeolite.

activity and further increase in TiO_2 was negatively affected.

3.2.3. Control Experiment

A preliminary study was carried out to investigate the role of catalyst under both silent (mechanical stirring only) and ultrasonic reaction. The adsorption study without the presence of ultrasonic irradiation was carried out to check the adsorption capacity of 0.4% Fe/15% TiO_2 -NaY catalyst for amaranth dye under continuous mechanical stirring for 120 min. The experimental runs were at an initial dye concentration of 10 mg/L, a catalyst loading of 1.5 g/L and at original pH of the dye solution. The results presented in **Figure 7** showed that only 4% of amaranth dye was adsorbed after 120 min of continuous stirring.

The decolorization efficiency under ultrasonic irradiation without the presence of catalyst was also investigated under the same reaction condition and the efficiency of the process was only about 12%. This low process efficiency was mainly ascribed to the limited generation of the hydroxyl radicals by the dissociation of water molecules during the ultrasonic reaction. In addition, Mahamuni *et al.* [18] suggested that the recombination of the $\cdot\text{OH}$ radicals within the cavity during the sonolysis process could eliminate the generation of the active species thus reduce the efficiency of the sonolysis process.

On the other hand, the decolorization efficiency visibly increased after the addition of catalyst under ultrasonic irradiation *i.e.* 17.4%, 30%, 68% and 76% for PTO (potassium titanium oxalate) calcined at 550°C, 0.4% Fe-NaY, 15% TiO_2 -NaY and 0.4% Fe/15% TiO_2 -NaY, respectively. The synergistic between the catalysts and the ultrasonic process led to increase the production of more hydroxyl radicals and enhance the decolorization efficiency. From **Figure 7**, it is clear that the incorporation

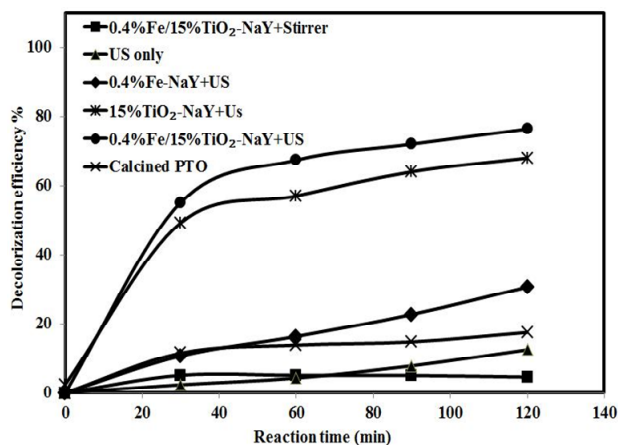


Figure 7. Preliminary study for the decolorization of amaranth dye under various conditions.

of Fe (III) and Ti species with zeolite could enhance the decolorization efficiency of amaranth as compared to that of 0.4 % Fe-NaY and 15% TiO₂-NaY catalysts.

3.2.4. Effect of pH

The effect of reaction acidity on the sonocatalytic degradation of amaranth was investigated within the pH range of 2.5 to 9.0 under ultrasonic reaction and the results are present in **Figure 8**. Before starting the sonocatalytic reaction, all the reactions were adjusted to the desire pH using 0.1 M NaOH or HCl with an initial dye concentration of 10 mg/L, 0.65 mM of H₂O₂ and 1.5 g/L catalyst loading for up to 120 min. It was noticed that the decolorization efficiency of the catalyst in the first 60 min was increased from 9% to 76% for pH 2.5 and 5.5, respectively. After longer reaction time, the color removal at different pH diminished and the reaction was almost complete with decolorization efficiency of about 98% for pH ranging from 3.5 to 9.0. Meanwhile, very low sonocatalytic activity of about 22.4% was obtained at the acidic condition of pH 2.5 after 120 min of reaction. The potassium (K) which was originally exists in the chemical structure of the titanium precursor was the reason behind this low catalytic activity at pH 2.5. The trace of such highly basic element exists at the catalyst in addition to the Fe and Ti will significantly affect the environment of the catalyst surface. Huang *et al.* [2] reported that the decolorization efficiency for methyl orange dye using Pt/TiO₂-zeolite catalyst was higher in high acidic condition.

An experiment run was carried out to investigate the effect of titanium precursor on the decolorization efficiency of amaranth at pH value of 2.5. The TiO₂ precursor (potassium titanium oxalate) used in this study was replaced with tetrabutyl orthotitanate using the same preparation method used in this study and the produced catalyst was denoted as 0.4% Fe/15% TBT-NaY. The dark experiment run showed an adsorption rate of 68% after 30 min of mechanical stirring without ultrasonic irradiation. However, the absorbed dye was desorbed

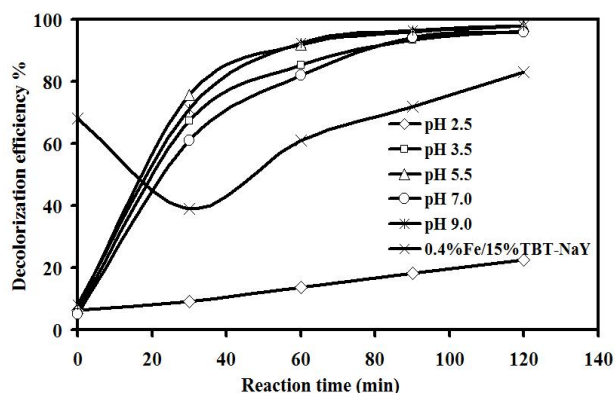


Figure 8. Effect of pH on decolorization efficiency of amaranth.

from the catalyst surface at the beginning of ultrasonic reaction due to the mechanical vibration provided by ultrasonic. The catalytic activity was 83% after 120 min of reaction without any addition of H₂O₂. It was clear that this large difference in catalytic activity between the original catalyst 0.4% Fe/15% TiO₂-NaY and 0.4% Fe/15% TBT-NaY at pH 2.5 was ascribed to the difference in chemical nature of TiO₂ precursor.

It is important to highlight that the zero point charge of the catalyst is depend on dispersion nature and the difference in catalyst diameter [6]. Furthermore, the surface properties are affected by the synergistic between Fe, TiO₂ and zeolite in addition to the trace of potassium oxide. This properties is complicated to be understand due the different component interact together. As a result, one can observe that the synthesized catalyst had high catalytic activity in a wide range of pH from 3.5 to 9.0 which could affect by the chemical nature of the catalyst.

3.2.5. Effect of Catalyst Loading

The decolorization efficiency of amaranth was demonstrated to obtain the optimum loading with respect to the amount of catalyst used from 1.0 to 2.5 g/L at an initial dye concentration of 10 mg/L, 0.65 mM of H₂O₂ and pH of 5.5 for up to 120 min. In **Figure 9**, it was notice that the difference in catalytic activity with different loading of catalyst was insignificant after 120 min of reaction and the activity was about 98% for the catalyst loadings variation from 1.0 to 2.5 g/L. This behavior could be attributed to the synergistic effect between the heterogeneous catalyst and the ultrasonic irradiation that provide mechanical mixing between the generated radicals and the dye molecules which enhance the catalytic activity [6]. However, there was a significant difference in decolorization efficiency at the first 30 min. The catalytic efficiency was found to increase with increasing catalyst loading to about 83% at catalyst loading of 2.0 g/L. Further increase in the amount of catalyst up to 2.5 g/L caused an activity drop to 74%.

The difference in sonocatalytic activity with different loading of catalyst at the first 30 min of reaction was

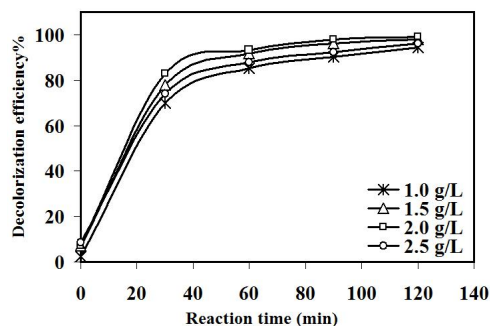


Figure 9. Effect of catalyst loading on decolorization efficiency of amaranth.

ascribed to multiple reason such as increase the number of the active sites of such catalyst that generate more $\cdot\text{OH}$ radicals during the sonocatalytic reaction. Furthermore, the presence of Fe ions provided higher decomposition rate for H_2O_2 to generate more hydroxyl radicals during the reaction [22]. Therefore, the reaction becomes faster with increasing the time of reaction. As such, the difference in catalytic activity with different loading of catalyst was diminished after 120 min of reaction. Wang *et al.* [23] reported that the optimum amount of catalyst loading for the Fe doped TiO_2 was 1 g/L for the degradation of azo fuchsine under ultrasonic reaction. Meanwhile, Zhong *et al.* [24] reported that the maximum catalyst loading of $\text{Fe}_2\text{O}_3/\text{Al}_2\text{O}_3$ for the sonocatalytic degradation of acid orange 7 was 0.3 g/L. As a conclusion, the optimal amount of catalyst loading varied depending on the process conditions, the nature of dye molecules and the properties of catalyst.

3.2.6. Effect of H_2O_2 Concentration

The decolorization efficiency of amaranth dye as a function of different H_2O_2 concentration was investigated at initial dye concentration of 10 mg/L, 2.0 g/L of catalyst loading, original pH of the dye about 5.5 and with different concentrations of H_2O_2 from (0.32 - 2.62) mM. The decolorization efficiency was found to increase from 72 % to 83 % at the first 30 min with increasing the concentration of H_2O_2 from 0.32 to 0.65 mM as presented in **Figure 10**. However, by increasing the concentration of H_2O_2 above 0.65 mM, the decolorization efficiency was decreased to 69% at 2.61 mM of H_2O_2 concentration. This behavior could be ascribed to the excess amount of H_2O_2 added to the reaction solution that led to the generation of hydroperoxyl radicals ($\text{HO}_2\cdot$) which was considered as the less reactive radicals compared to $\cdot\text{OH}$ radicals [25]. Aravindhan *et al.* [26] reported that excess amount of H_2O_2 added into the reaction system can negatively affect the efficiency of the process due to the scavenging of $\cdot\text{OH}$.

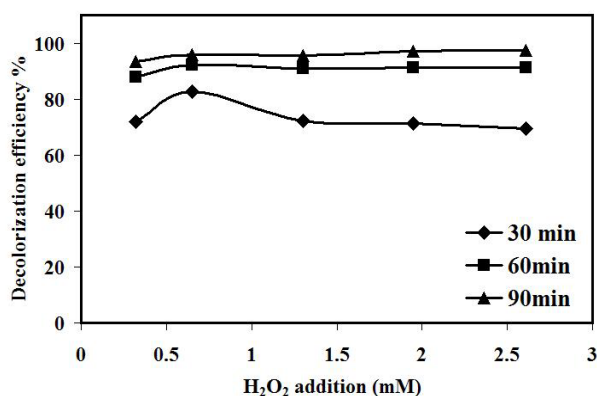


Figure 10. Effect of H_2O_2 on decolorization efficiency amaranth.

Pang *et al.* [27] reported that the optimum amount of H_2O_2 needed to add into the ultrasonic reaction is depends on the type of the organic compound to be degraded and the ultrasonic operating condition. However, the presence of heterogeneous catalyst in synergistic with ultrasonic irradiation can be consider another factor that effect on the amount of H_2O_2 added into the reaction. In section 3.2.2 the sonocatalytic activity of 0.4% Fe/15% TiO_2 -NaY without the addition of H_2O_2 was 74% thus, only 0.65 mM was needed to enhance the catalytic activity to 97% after 120 min of reaction and that no desirable effect in the color removal was observed with the addition of higher concentration of H_2O_2 .

3.2.7. Effect of Initial Dye Concentration

The decolorization efficiency of 0.4% Fe/15% TiO_2 -NaY catalyst as a function of initial dye concentration was also investigated. The experimental runs were carried at 2 g/L of catalyst loading, original pH of the dye solution *i.e.* about 5.5 and 0.65 mM of H_2O_2 . It was noted in **Figure 11** that nearly complete decolorization was obtained at the end of the reaction at different initial dye concentrations from 10 to 100 mg/L. However, the rate of decolorization in the first 30 min of reaction was directly proportional to the decrease in initial dye concentration.

As the time of reaction was further increased, the color removal was relatively fast for the case of 30 mg/L of initial dye concentration. This behavior can be explained based on the collision theory [28]. With increasing the concentration of dye molecules per unit volume of reaction, the chance of collisions between these reactants molecules increased thus, the decolorization efficiency steadily increased. Above the optimum value of 30 mg/L of the initial dye concentration, the decolorization efficiency after 60 min decreased from 100% to 85% for 30 and 100 mg/L of initial dye concentration, respectively. Jamalluddin Abdullah [29] reported the low decolorization efficiency with increasing the concentration of dye could be affected by the mutual screening between the

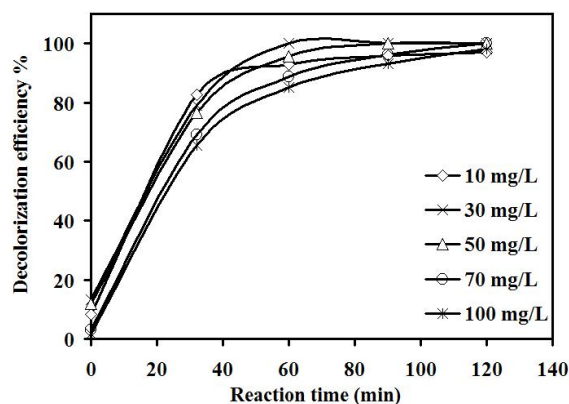


Figure 11. Effect of initial dye concentration on decolorization efficiency of amaranth.

organic dyes molecules at higher concentration of dye. However, with increasing the time of reaction more decolorization rate was observed and this mutual screening with higher dye concentration was significant only in earlier time of reaction.

It was found that the leaching of Fe^{3+} ions increased with increasing the concentration of dye molecules due to the generation of more acidic-by products that were formed during the reaction thus enhance the dissolving of Fe^{3+} ions during the reaction. The concentrations of Fe^{3+} found in the solution after 120 min of reaction were 0.011, 0.017, 0.033, 0.051 and 0.06 mg/L for 10, 30, 50, 70 and 100 mg/L, respectively. The more Fe^{3+} leached out from the catalyst, the more loss in active sites of catalyst was expected [30]. However, this small amount of Fe^{3+} ions separated from the catalyst did not affect the decolorization efficiency even for the high concentration of dye as it was clear from **Figure 11**.

Our previous report [5] investigates the degradation of amaranth using the heterogeneous catalyst of Fe loaded on encapsulated TiO_2 . The higher decolorization efficiency of amaranth was 98% at 10 mg/L initial concentration, 2.5 pH, 0.2 M H_2O_2 and 2 g/L catalyst loading. However, in this catalyst the maximum decolorization efficiency was obtained at 30 mg/L initial dye concentration, 5.5 pH, 0.65 mM H_2O_2 and 2 g/L catalyst loading. The difference in optimum conditions between the two catalysts was significant especially for amount of H_2O_2 and pH of reaction solution. It seems that position of TiO_2 with respect to zeolite structure, preparation method and the amount of TiO_2 affect extremely on chemical environment of the catalyst and consequently effect on the optimum condition of the reaction.

4. Conclusion

A heterogeneous catalyst was successfully synthesized in one simple step using a wet impregnation method. Incorporation between Ti and Fe into the zeolite successfully enhanced the sonocatalytic reaction. The XRD results showed that chemical nature of titanium precursor affected significantly on the crystallinity of the catalyst. The AFM results showed a significant reduction in the surface roughness of the catalyst after the loading of 15% TiO_2 and 0.4% Fe/15% TiO_2 into the zeolite. Effects of different reaction variables were elucidated to achieve the higher decolorization of amaranth. The maximum decolorization efficiency of the 0.4% Fe/15% TiO_2 -NaY was 100% at an initial dye concentration of 30 mg/L, 2 g/L of catalyst loading, natural pH of 5.5 and H_2O_2 concentration of 0.65 mM.

5. Acknowledgements

The Research University grant from Universiti Sains Malaysia to support this work is gratefully acknowledged.

ed.

REFERENCES

- [1] H. Wang, Y. Shen, C. Shen, Y. Wen and H. Li, "Enhanced Adsorption of Dye on Magnetic Fe_3O_4 via HCl-Assisted Sonication Pretreatment," *Desalination*, Vol. 284, 2012, pp. 122-127. doi:10.1016/j.desal.2011.08.045
- [2] M. Huang, C. Xu, Z. Wu, Y. Huang, J. Lin and J. Wu, "Photocatalytic Discolorization of Methyl Orange Solution by Pt Modified TiO_2 Loaded on Natural Zeolite," *Dyes and Pigments*, Vol. 77, No. 2, 2008, pp. 327-334. doi:10.1016/j.dyepig.2007.01.026
- [3] S. S. Rayalu, N. Dubey, R. V. Chatti, M. V. Joshi, N. K. Labhsetwar and S. Devotta, "Effect of Heteropolyacid and Its Route of Incorporation on the Photocatalytic Properties of Zeolite-Based Materials," *Current Science*, Vol. 93, No. 10, 2007, pp. 1376-1382.
- [4] A. N. Soon and B. H. Hameed, "Heterogeneous Catalytic Treatment of Synthetic Dyes in Aqueous Media Using Fenton and Photo-Assisted Fenton Process," *Desalination*, Vol. 269, No. 1-3, 2011, pp. 1-16. doi:10.1016/j.desal.2010.11.002
- [5] A. H. Alwash, A. Z. Abdullah and N. Ismail, "Zeolite Y Encapsulated with Fe- TiO_2 for Ultrasound-Assisted Degradation of Amaranth Dye in Water," *Journal of Hazardous Materials*, Vol. 233-234, 2012, pp. 184-193. doi:10.1016/j.jhazmat.2012.07.021
- [6] Y. L. Pang, S. Bhatia and A. Z. Abdullah, "Process Behavior of TiO_2 Nanotube-Enhanced Sonocatalytic Degradation of Rhodamine B in Aqueous Solution," *Separation and Purification Technology*, Vol. 77, No. 3, 2011, pp. 331-338. doi:10.1016/j.seppur.2010.12.023
- [7] R. J. Tayade, R. G. Kulkarni and R. V. Jasra, "Enhanced Photocatalytic Activity of TiO_2 -Coated NaY and HY Zeolites for the Degradation of Methylene Blue in Water," *Industrial and Engineering Chemistry Research*, Vol. 46, No. 2, 2007, pp. 369-376. doi:10.1021/ie060641o
- [8] X. Li, B. Shen and C. Xu, "Interaction of Titanium and Iron Oxide with ZSM-5 to Tune the Catalytic Cracking of Hydrocarbons," *Applied Catalysis A: General*, Vol. 375, No. 2, 2010, pp. 222-229. doi:10.1016/j.apcata.2009.12.033
- [9] P. Castaño, B. Pawelec, J. L. G. Fierro, J. M. Arandes and J. Bilbao, "Aromatics Reduction of Pyrolysis Gasoline (PyGas) over HY-Supported Transition Metal Catalysts," *Applied Catalysis A: General*, Vol. 315, 2006, pp. 101-113. doi:10.1016/j.apcata.2006.09.009
- [10] C. Wang, H. Shi and Y. Li, "Synthesis and Characteristics of Natural Zeolite Supported Fe^{3+} - TiO_2 Photocatalysts," *Applied Surface Science*, Vol. 257, No. 15, 2011, pp. 6873-6877. doi:10.1016/j.apsusc.2011.03.021
- [11] C. C. Wang, C. K. Lee, M. D. Lyu and L. C. Juang, "Photocatalytic Degradation of C.I. Basic Violet 10 Using TiO_2 Catalysts Supported by Y Zeolite: An Investigation of the Effects of Operational Parameters," *Dyes and Pigments*, Vol. 76, No. 3, 2008, pp. 817-824. doi:10.1016/j.dyepig.2007.02.004
- [12] A. Z. Abdullah and P. Y. Ling, "Heat Treatment Effects

- on the Characteristics and Sonocatalytic Performance of TiO₂ in the Degradation of organic Dyes in Aqueous Solution,” *Journal of Hazardous Materials*, Vol. 173, No. 1-3, 2010, pp. 159-167.
[doi:10.1016/j.jhazmat.2009.08.060](https://doi.org/10.1016/j.jhazmat.2009.08.060)
- [13] H. Hassan and B. H. Hameed, “Oxidative Decolorization of Acid Red 1 Solutions by Fe-Zeolite Y Type Catalyst,” *Desalination*, Vol. 276, No. 1-3, 2011, pp. 45-52.
[doi:10.1016/j.desal.2011.03.018](https://doi.org/10.1016/j.desal.2011.03.018)
- [14] G. Li, “FT-IR Studies of Zeolite Materials: Characterization and Environmental Applications,” The University of Iowa’s Institutional Repository, 2005.
- [15] C. Li and Z. Wu, “Microporous Materials Characterized by Vibrational Spectroscopies,” In: S. M. Auerbach, K. A. Carrado and P. K. Dutta, Eds., *Handbook of Zeolite Science and Technology*, CRC Press, Boca Raton 2003, pp. 423-514. [doi:10.1201/9780203911167.ch11](https://doi.org/10.1201/9780203911167.ch11)
- [16] M. Nikazar, K. Gholivand and K. Mahanpoor, “Photocatalytic Degradation of Azo Dye Acid Red 114 in Water with TiO₂ Supported on Clinoptilolite as a Catalyst,” *Desalination*, Vol. 219, No. 1, 2008, pp. 293-300.
[doi:10.1016/j.desal.2007.02.035](https://doi.org/10.1016/j.desal.2007.02.035)
- [17] H. G. Karge, “Characterization by Infrared Spectroscopy,” *Microporous Mesoporous Materials*, Vol. 22, No. 4-6, 1998, pp. 547-549.
[doi:10.1016/S1387-1811\(98\)80021-8](https://doi.org/10.1016/S1387-1811(98)80021-8)
- [18] N. N. Mahamuni and A. B. Pandit, “Effect of Additives on Ultrasonic Degradation of Phenol,” *Ultrasonic Sonochemistry*, Vol. 13, No. 2, 2006, pp. 165-174.
[doi:10.1016/j.ultsonch.2005.01.004](https://doi.org/10.1016/j.ultsonch.2005.01.004)
- [19] F. A. Q. Ortíz, J. T. Valenzuela and C. A. R. Reyes, “Zeolitisation of Neogene Sedimentary and Pyroclastic Rocks Exposed in Paipa (Boyacá), in the Colombian Andes: Simulating Their Natural Formation Conditions,” *Earth Sciences Research Journal*, Vol. 15, No. 2, 2011, pp. 89-100.
- [20] H. Faghihian and A. Bahranifard, “Application of TiO₂-Zeolite as Photocatalyst for Photodegradation of Some Organic Pollutants,” *Iranian Journal of Catalysis*, Vol. 1, No. 1, 2011, pp. 45-50.
- [21] C. Bajamundi, M. Dalida, K. Wantala, P. Khemthong and N. Grisdanurak, “Effect of Fe³⁺ Doping on the Performance of TiO₂ Mechanocoated Alumina Bead Photocatalysts,” *Korean Journal of Chemical Engineering*, Vol. 28, No. 8, 2011, pp. 1688-1692.
[doi:10.1007/s11814-011-0031-7](https://doi.org/10.1007/s11814-011-0031-7)
- [22] J. Herney-Ramirez, M. A. Vicente and L. M. Madeira, “Heterogeneous Photo-Fenton Oxidation with Pillared Clay-Based Catalysts for Wastewater Treatment: A Review,” *Applied Catalysis B: Environmental*, Vol. 98, No. 1-2, 2010, pp. 10-26. [doi:10.1016/j.apcatb.2010.05.004](https://doi.org/10.1016/j.apcatb.2010.05.004)
- [23] J. Wang, W. Sun, Z. Zhang, Z. Jiang, X. Wang, R. Xu, R. Li and X. Zhang, “Preparation of Fe-Doped Mixed Crystalline TiO₂ Catalyst and Investigation of Its Sonocatalytic Activity during Degradation of Azo Fuchsine under Ultrasonic Irradiation,” *Journal of Colloid and Interface Science*, Vol. 320, No. 1, 2008, pp. 202-209.
[doi:10.1016/j.jcis.2007.12.013](https://doi.org/10.1016/j.jcis.2007.12.013)
- [24] X. Zhong, L. Xiang, S. Royer, S. Valange, J. Barrault and H. Zhang, “Degradation of C.I. Acid Orange 7 by Heterogeneous Fenton Oxidation in Combination with Ultrasonic Irradiation,” *Journal of Chemical Technology & Biotechnology*, Vol. 86, No. 7, 2011, pp. 970-977.
- [25] M. Neamtu, C. Zaharia, C. Catrinescu, A. Yediler, M. Macoveanu and A. Kettrup, “Fe-Exchanged Y Zeolite as Catalyst for Wet Peroxide Oxidation of Reactive Azo Dye Procion Marine H-EXL,” *Applied Catalysis B: Environmental*, Vol. 48, No. 4, 2004, pp. 287-294.
[doi:10.1016/j.apcatb.2003.11.005](https://doi.org/10.1016/j.apcatb.2003.11.005)
- [26] R. Aravindhan, N. N. Fathima, J. R. Rao and B. U. Nair, “Wet Oxidation of Acid Brown Dye by Hydrogen Peroxide Using Heterogeneous Catalyst Mn-Salen-Y Zeolite: A Potential Catalyst,” *Journal of Hazardous Materials*, Vol. 138, No. 1, 2006, pp. 152-159.
[doi:10.1016/j.jhazmat.2006.05.052](https://doi.org/10.1016/j.jhazmat.2006.05.052)
- [27] Y. L. Pang, A. Z. Abdullah and S. Bhatia, “Review on Sonochemical Methods in the Presence of Catalysts and Chemical Additives for Treatment of Organic Pollutants in Wastewater,” *Desalination*, Vol. 277, No. 1-3, 2011, pp. 1-14. [doi:10.1016/j.desal.2011.04.049](https://doi.org/10.1016/j.desal.2011.04.049)
- [28] M. B. Kasiri, H. Aleboyeh and A. Aleboyeh, “Degradation of Acid Blue 74 Using Fe-ZSM5 Zeolite as a Heterogeneous Photo-Fenton Catalyst,” *Applied Catalysis B: Environmental*, Vol. 84, No. 1-2, 2008, pp. 9-15.
[doi:10.1016/j.apcatb.2008.02.024](https://doi.org/10.1016/j.apcatb.2008.02.024)
- [29] N. A. Jamalluddin and A. Z. Abdullah, “Reactive Dye Degradation by Combined Fe(III)/TiO₂ Catalyst and Ultrasonic Irradiation: Effect of Fe(III) Loading and Calcination Temperature,” *Ultrasonic Sonochemistry*, Vol. 18, No. 2, 2011, pp. 669-678.
[doi:10.1016/j.ultsonch.2010.09.004](https://doi.org/10.1016/j.ultsonch.2010.09.004)
- [30] N. A. Jamalluddin and Z. A. Ahmad, “Effect of pH and Catalyst Dosage on the Leaching of Fe from Fe(III) Doped Zeolite Y Used for Sonocatalytic Degradation of Acid Red B,” *Research Journal of Chemistry and Environment*, Vol. 15, No. 2, 2011, pp. 860-865.